SAND2018-0378J

High-pressure-assisted X-ray-induced damage as a new route for materials synthesis.

Egor Evlyukhin[1*], Eunja Kim[1], David Goldberger[1], Petrika Cifligu[1], Philippe F. Weck[2], Michael Pravica[1].

[1]*High Pressure Science and Engineering Center (HiPSEC) and Department of Physics and Astronomy, University of Nevada Las Vegas (UNLV), Las Vegas, Nevada USA, 89154-4002.*

[2]*Sandia National Laboratories, Albuquerque, New Mexico USA, 87185.*

X-ray radiation induced damage has been known for decades and has largely been viewed as a tremendous nuisance; e.g., most X-ray–related studies of organic and inorganic materials suffer X-ray damage to varying degrees. Although, recent theoretical and experimental investigation of the response of simple chemical systems to X-rays offered better understanding of the mechanistic details of X-ray induced damage, the question about useful applicability of this technique is still unclear. Here we experimentally demonstrate that by tuning pressure and X-rays energy, the radiation induced damage can be controlled and used for synthesis of novel materials. We show that powdered cesium oxalate monohydrate at pressure ≤0.5 GPa and under X-ray radiation at energies around K-edge of cesium undergoes molecular and structural transformation and that the final product exhibits a new type of crystal structure which previously has not been observed. Additionally, based on cascades of ultrafast electronic relaxation steps triggered by absorption of X-ray photons we propose a model explaining the X-ray induced damage of multitype bounded matter.

Electronic excitation of atoms and molecules and subsequent relaxation processes are the main factors which cause X-ray induced radiation damage of matter[1-6]. Recent investigations of electronic decay processes induced by X-rays in loosely bound chemical systems demonstrated tremendous progress in understanding the sequence of events that leads to radiation induced damage[1,7-11]. Basically, absorption of an X-ray photon by an atom excites a K-shell electron to a bound state[2,3] or removes it from the host to the continuum[1] and initiates a cascade of relaxation processes. The origin and sequence of relaxation processes strongly depend upon the chemical composition and environment of the irradiated system[10,12-14]. Recently, the role of metal ions in X-ray-induced photochemistry has been studied from the theoretical point of view[1]. It has been shown that absorption of X-rays by microsolvated Mg^{+2} results in cascade of ultrafast electronic relaxation steps that include both intra- and intermolecular processes. At the end of this cascade the metal reverts to its original oxidation state whereas the surrounding environment becomes multiply ionized and contains a large amount of radicals and slow electrons. Such high capability of chemical systems to absorb X-ray photons which leads to distortion of molecular structure makes the study of these systems using X-ray crystallographic techniques problematic. Thereby, understanding the mechanisms of X-ray induced damage and the possibility to control this damage will be extremely useful for: (i) understanding the response of chemical systems to ionizing radiation, (ii) development of novel synthetic methods to create unique and potentially useful materials, and (iii) enabling more thorough analysis of their properties.

In spite of accumulated knowledge mentioned above, the X-rays properties in terms of material synthesis are still unclear. Moreover little is known about the role of high pressure and radiation energy in X-ray induced photochemistry. In what follows we present an experimental study of the X-ray induced chemical and structural transformation of powdered cesium oxalate hydrate ($Cs_2C_2H_2O_5$) at ambient and high pressure (≤0.5 GPa) by means of X-ray Diffraction (XRD). We found that X-rays with high pressure assistance opens new reaction pathways which differ from those activated by conventional methods[15] and drives the synthesis of novel materials with the formation of unique crystal structure properties. Additionally, we propose a model of X-ray induced photochemistry that shows how the photoabsorption by metal species triggers the cascade of electronic relaxation processes which results in multiple ionization of surrounding environment, even in cases in which metal reverts to its original charge state before the absorption of an X-ray photon.

Results

To investigate the X-ray induced damage and role of high pressure we considered a powder of $Cs_2C_2H_2O_5$ as a studying system. $Cs_2C_2H_2O_5$ was loaded into a diamond anvil cell (DAC) and irradiated with monochromatic X-rays of selected energies which were above or below the K-edge of cesium (35.987 keV)[16] at ambient and at high pressure (≤0.5 GPa). Fig.1a displays *in situ* XRD patterns of $Cs_2C_2H_2O_5$ at ambient pressure after varying X-ray irradiation times at 36 keV. The first XRD pattern obtained during one minute of irradiation matches the previously reported monoclinic crystal structure of cesium oxalate hydrate[17] with *C2/c* space group (vertical bars in Fig1a). Upon further irradiation, the XRD peak intensities decrease indicating distortion of electron density distribution (XRD patterns 5 - 40 min in Fig1a). Nevertheless, even after 40 min of X-ray irradiation, the XRD peak positions do not change and no new peaks are observed demonstrating that X-ray exposed $Cs_2C_2H_2O_5$ at ambient pressure does not undergo any structural transformations. On the other hand, the picture dramatically changes when high pressure is applied. Fig.1b demonstrates the *in situ* XRD patterns of $Cs_2C_2H_2O_5$ at 0.3 GPa before and after different periods of X-ray irradiation at 36 keV. It is evident from Fig.1b that after 2 min of X-ray irradiation, the peak intensities significantly decrease whereas the peak positions remain the same. However, significant changes in the XRD pattern are observed immediately after the third minute of X-ray irradiation. Two peaks at 6.03º and 6.25º merge into one broad peak at 6.16º. Upon further irradiation up to 10 min, the XRD pattern changes completely. Many of the peaks observed in the initial XRD pattern disappear and a new peak at 10.71º forms. These dramatic changes indicate that irradiated $Cs_2C_2H_2O_5$ at 0.3 GPa undergoes a significant structural transformation. Continued X-ray irradiation up to 40 min does not significantly modify the XRD pattern with exception of the formation of a new small peak at

7.13º indicating that major structural transformation happen during first 10 minutes of irradiation.

Our Raman spectroscopic studies showed that the final product after 40 min of X-ray irradiation at pressure 0.3 GPa consists of different types of cesium-oxygen based compounds[15,18-21] (See Supplementary Fig.2). These are, cesium peroxide (Cs_2O_2)[15,18], cesium superoxide (CsO_2)[15,18-21] and cesium formate ($CHCsO_2$)[22]. Based on these spectroscopic evidences, we propose two candidate structures to elucidate our final product. They are: a previously reported orthorhombic crystal structure of cesium peroxide[23] with a space group *Immm* (blue vertical bars in Fig.1b) and a cubic crystalline structure of cesium superoxide[24] with a space group *Fm-3m* using lattice parameter 7.84 Å (red vertical bars in Fig.1b). Both of these candidate structures contain peaks that are observed in the XRD pattern of X-ray irradiated $Cs_2C_2H_2O_5$ at 0.3 GPa and provide evidence for the final disposition and composition of our product.

The next question we address in this *Letter* pertains to the energy dependence of X-ray irradiation induced damage[6]. Samples of $Cs_2C_2H_2O_5$ pressurized in a DAC up to 0.3 GPa were irradiated with X-rays in the 32 - 42 keV energy range with 3 keV steps. After 40 min of irradiation at each energy, the same crystal structure was obtained (Supplementary Fig.3) demonstrating that the structural transformation path does not depend upon the X-ray energy. Nerveless, to quantify X-ray induced structural transformations as a function of irradiation energy, we analyzed the change in integrated area underneath selected XRD peaks before and after irradiation. Fig.2a demonstrates selected XRD peaks in d-space of $Cs_2C_2H_2O_5$ before and after 40 min of X-ray irradiation. The transformation yield (*TY*) as function of X-ray energy is defined as

$$TY = \frac{Area_{final} \times 100\%}{Area_{int}} \qquad (1),$$

where $Area_{int}$ and $Area_{final}$ are respectively the integrated areas of selected peaks before and after 40 min of irradiation. The *TY* as a function of X-ray energy is presented in Fig.2b. As seen in the figure, the maximum X-ray induced chemical and structural transformation (78.7 %) is achieved when the samples were irradiated at 36 keV, which is slightly above the K-edge of cesium (35.987 keV) verifying that excited K-shell electrons play an important role in X-ray induced damage.

Discussion

To understand the nature of X-ray energy- and pressure- dependence of irradiation-induced damage discussed above, we propose a new model of X-ray induced damage in multitype bounded matter. Fig.3 displays the schematic representation of electronic decay processes triggered by absorption of one photon by cesium atoms with energies less than the energy of the cesium K-edge but higher than the energy of cesium L-edge. Absorption of an X-ray photon by one cesium atom excites a K-shell electron to a bound state[2,3] and initiates a cascade of relaxation steps. There are three possible decay processes which compete with each other depending on the ionization potential of created exited states[11]: (i) Auger decay[25] during which an electron with a characteristic energy is emitted by Cs^+ which, in turn, accumulates a positive charge Cs^{+2}; (ii) intermolecular Coulombic decay (ICD)[26] when an excited cesium atom decays by transferring its excess energy only to a loosely bound water molecule[8] that would then emit a low-energy electron ($(H_2O)^+$); (iii) radiative decay during which the excited cesium atom decays via emission of characteristic X-rays (hν). After ICD or radiative decay, an excited cesium atom reverts to its original charge state, whereas Auger decay triggers additional cascades of relaxation steps to bring Cs^{+2} back to its initial charge state. These additional steps entail radiative decay and/or ICD[2,3] which are then followed by electron-transfer-mediated-decay (ETMD). During ETMD, neighboring anions/molecules of $(C_2O_4)^{2-}$ or (H_2O) donate electrons to Cs^{+2} and the excess energy ionizes the donor itself (ETMD(1)), or another molecule (ETMD(2)), causing the cesium atom to revert to its initial charge state, and ionizing the surrounding environment. The corresponding model changes when the X-ray photon energy is above the cesium K-edge. Fig.4 presents the schematic representation of electronic decay processes triggered by absorption of one X-ray photon by a cesium atom with energies slightly (10-100 eV) or greatly (≥ 1 keV) above the cesium K-edge energy. Absorption of an X-ray photon by one Cs^+ removes a K-shell electron, promoting it into the continuum[1,25]. This changes the charge state of cesium to Cs^{+2}. The created photoelectron may secondarily ionize the surrounding environment depending on its energy[27]. The following chain of relaxation steps is similar to the previously discussed model with the exception of relaxation cascades paths followed after the first Auger decay. There are three possible ETMD channels following Auger decay: (i) a $(C_2O_4)^{2-}$ anion donates 2 electrons to Cs^{+3}; (ii) an (H_2O) molecule donates 2 electrons to Cs^{+3}; and (iii) a $(C_2O_4)^{2-}$ anion and (H_2O) molecule donate one electron each to Cs^{+3}. In all cases the absorption of one X-ray photon by cesium cations completely changes the surrounding environment (i.e. ionized/destabilized neighboring molecules/anions which will likely decompose[1], and a large concentration of slow or fast free electrons). Despite this myriad effects, structural transformations are only observed when high pressure is applied, verifying that reduced distances between molecules, even if they are already ionized, is a necessary condition for the formation of a new crystalline structure. Moreover, the *TY* maximum at X-ray energies slightly above cesium K-edge demonstrates that the concentration of slow photoelectrons is also a critical parameter in X-ray induced photochemistry.

In closing, we note that most living systems largely consist of biological molecules and that there are many theories that some of them may have originated in outer space under mildly high pressure conditions with a low dose of x-rays over many millions/billions of years. We feel that this study may provide us some insights into the mechanism of formation of some important biologically-related systems within the deepest reaches of outer space.

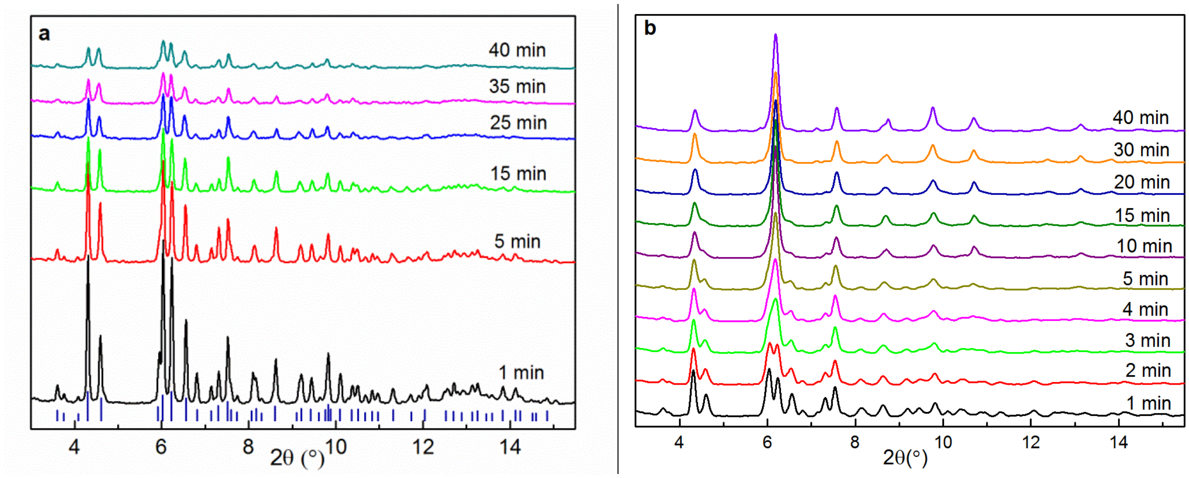

Figure 1| XRD patterns of cesium oxalate hydrate after different times of X-ray irradiation. **a**, $Cs_2C_2H_2O_5$ at ambient pressure; vertical bars indicate peak positions of the monoclinic crystal structure of cesium oxalate hydrate[17] (the full assignment of XRD pattern is presented in Supplementary Fig.1). **b**, $Cs_2C_2H_2O_5$ at 0.3 GPa; vertical blue bars indicate peak positions of the orthorhombic crystal structure of cesium peroxide[23] with a space group *Immm*, and vertical red bars correspond to the cubic crystal structure of cesium superoxide[24] with a space group *Fm-3m* using lattice parameter $a = 7.84$ Å.

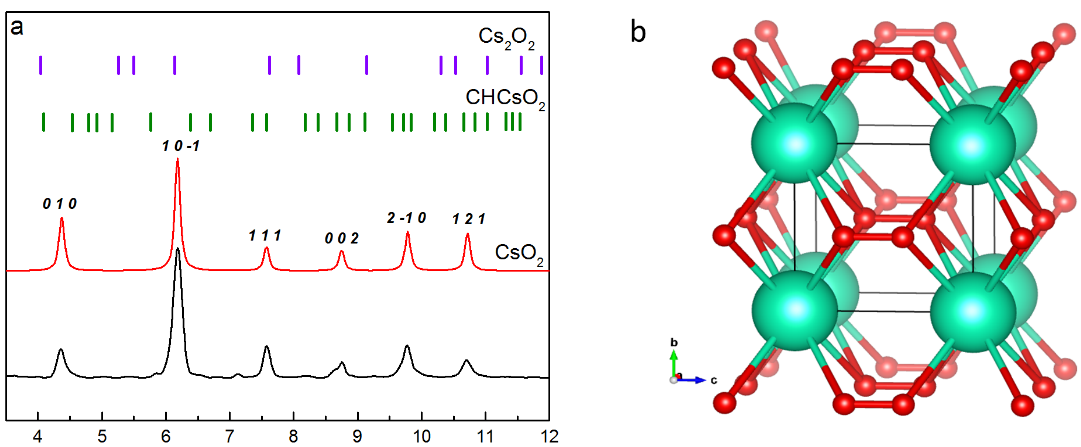

Figure 2| Characterization of structural properties of irradiated samples after 40 min of X-rays at 36 keV. a, XRD patterns of the final product and theoretically predicted crystal structure of CsO_2; vertical purple bars indicate peak positions of the orthorhombic crystal structure of cesium peroxide[23] with a space group *Immm* and vertical green bars correspond to the orthorhombic crystal structure of cesium formate[||]**???** with a space group *Pbcm*. **b,** Theoretically predicted crystal structure of CsO_2. Green and red spheres represent Cs and O atoms, respectively.

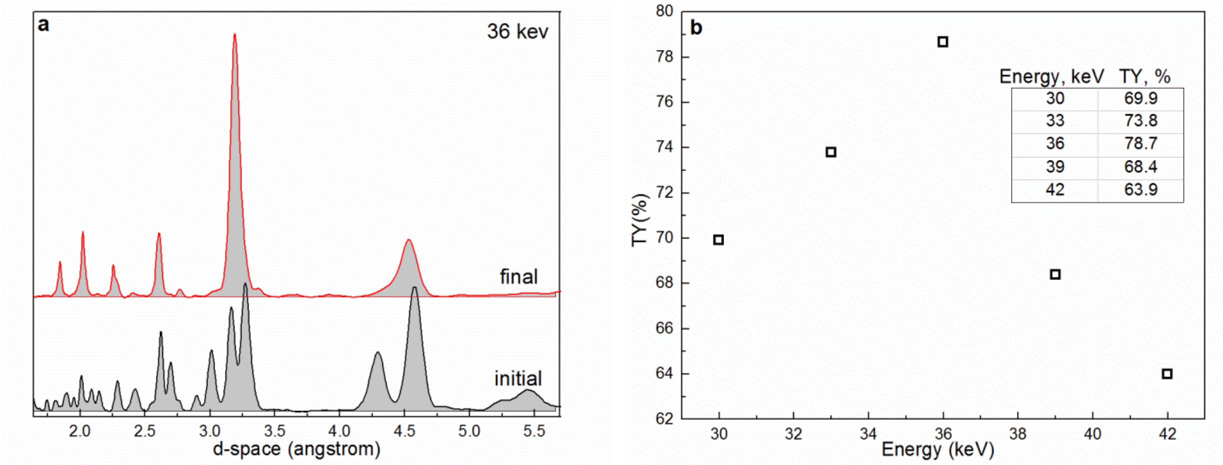

Figure 3| High-pressure assisted X-ray induced transformation yield (*TY*) of cesium oxalate hydrate. a, Selected area (in grey) is presented in d-space (1.63 - 5.66 Å) plot of XRD patterns before (initial) and after 40 min (final) of X-ray irradiation of $Cs_2C_2H_2O_5$ at 0.3GPa. **b**, X-ray induced *TY* of $Cs_2C_2H_2O_5$ at 0.3 GPa as a function of X-ray photon energy.

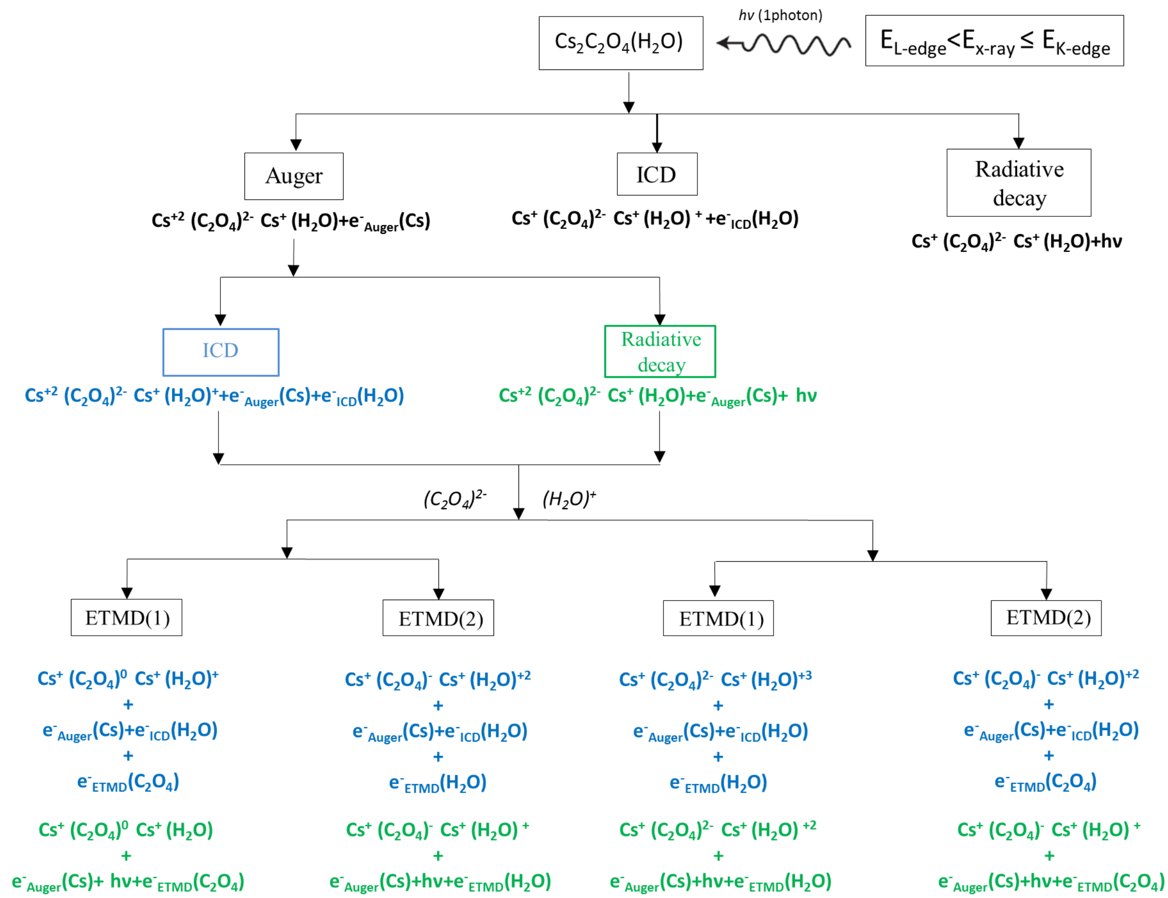

Figure 4| Schematic illustration of the electronic decay processes induced by absorption of one X-ray photon with energy less than K-edge of Cs but higher than L-edge of Cs by one $Cs_2C_2H_2O_5$ molecule. After each relaxation step, the change of the molecular oxidation states with the type of excited free electrons is presented. Different colors correspond to different relaxation paths.

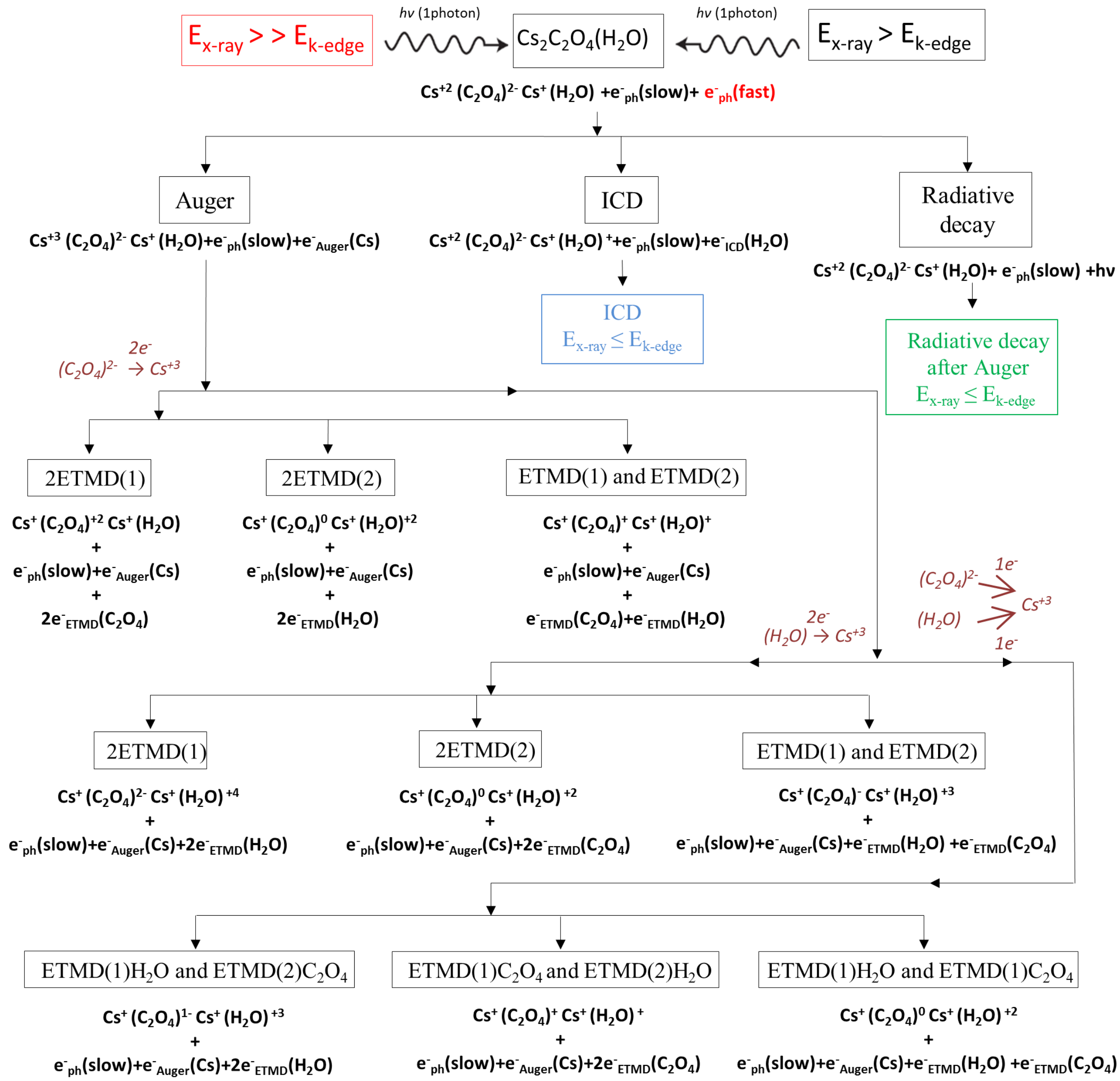

Figure 5| Schematic illustration of the electronic decay processes induced by absorption of one X-ray photon with energy slightly or far above the K-edge of Cs by one $Cs_2C_2H_2O_5$ molecule. After each relaxation step, the change of molecular oxidation states with the type of excited free electrons is presented. 2ETMD represents the relaxation process during which the $(C_2O_4)^{2-}$ or $(H_2O)^-$molecules donate two electrons to Cs^+. ETMD(x)A represent the relaxation process during which molecule A donates an electron to Cs^+, and the excess energy is used to ionize the donor itself (x=1) or another molecule (x=2).

Methods

Experimental details. All experiments were performed at the 16 BM-D beamline of the High Pressure Collaborative Access Team (HP-CAT) at the Advanced Photon Source. A tunable Si (111) double crystal in pseudo-channel-cut mode was used as a monochromator to filter "white" X-ray radiation and supply X-rays of fixed but settable energies. A symmetric-style diamond anvil cell (DAC) with 250 μm thick stainless-steel gaskets was used to confine and pressurize samples of powdered $Cs_2C_2H_2O_5$. The diamonds utilized each had culets ~300 μm in diameter. All $Cs_2C_2O_4$ samples (Sigma-Aldrich, purity > 99%) were loaded inside a glove box into a ~140 μm diameter hole that was drilled via electric discharge machining in the gasket center that was pre-indented to ~40 μm thickness. Due to the high reactivity of $Cs_2C_2O_4$ with moisture all investigated samples contained water molecules and every sample was identified as $Cs_2C_2H_2O_5$. A ruby ball was loaded with each sample for pressure measurement purposes to ensure that the sample remained at ambient pressure or pressurized at pressure ≤0.5 GPa. No pressure-transmitting medium was used in the experiments. All samples were irradiated with X-rays ranging in energy from 30 to 42 keV for 40 min at each energy. The horizontal and vertical full width half-maximum (FWHM) of the X-ray beam varied from 3.5 - 4.2 μm as the energy of the beam changed. Angular-dispersive X-ray diffraction patterns were collected every minute using a Pilatus® 1M pixel array detector. Note that between each minute of X-ray irradiation there was a 1 min gap which is the time required for the software to transform and save collected data. The diffraction patterns were integrated in 2-theta using the Dioptas® program, to produce intensity versus 2-theta plots. Raman spectra of samples confined and compressed in DAC at room temperature were measured using an ISA HR460® spectrometer with a Peltier-cooled CCD detector (Andor® 1024x128 pixels). An Ar ion multiline laser tuned to 532 nm served as the excitation source.

Data availability. The data supporting the findings of this study are available from the corresponding authors on reasonable request.

References

1. Stumpf, V., Gokhberg, K. & Cederbaum, L.S. The role of metal ions in X-ray-induced photochemistry. *Nature Chemistry* **8,** 237-241 (2016).
2. Gokhberg, K., Kolorenč, P., Kuleff, A.I. & Cederbaum, L.S. Site- and energy-selective slow-electron production through intermolecular Coulombic decay. *Nature* **505,** 661-663 (2013).
3. Trinter, F. *et al.* Resonant Auger decay driving intermolecular Coulombic decay in molecular dimers. *Nature* **505,** 664-666 (2013).
4. Jawad, H.H. & Watt, D.E. Physical Mechanism for Inactivation of Metallo-enzymes by Characteristic X-rays. *International Journal of Radiation Biology and Related Studies in Physics, Chemistry and Medicine* **50,** 665-674 (1986).
5. Carugo, O. & Carugo, K.D. When X-rays modify the protein structure: radiation damage at work. *Trends in Biochemical Sciences* **30,** 213-219 (2005).
6. Goldberger, D., Evlyukhin, E., Cifligu, P., Wang, Y. & Pravica, M. Measurement of the Energy and High-Pressure Dependence of X-ray-Induced Decomposition of Crystalline Strontium Oxalate. *The Journal of Physical Chemistry A* **121,** 7108-7113 (2017).
7. Thürmer, S. *et al.* On the nature and origin of dicationic, charge-separated species formed in liquid water on X-ray irradiation. *Nature Chemistry* **5,** 590-596 (2013).
8. Cederbaum, L.S., Zobeley, J. & Tarantelli, F. Giant Intermolecular Decay and Fragmentation of Clusters. *Physical Review Letters* **79,** 4778-4781 (1997).
9. Jahnke, T. Interatomic and intermolecular Coulombic decay: the coming of age story. *J. Phys. B: At. Mol. Opt. Phys.* **48,** 082001 (2015).
10. Jahnke, T. *et al.* Ultrafast energy transfer between water molecules. *Nature Physics* **6,** 139-142 (2010).
11. Zobeley, J., Santra, R. & Cederbaum, L.S. Electronic decay in weakly bound heteroclusters: Energy transfer versus electron transfer. *The Journal of Chemical Physics* **115,** 5076-5088 (2001).
12. Marsalek, O. *et al.* Chasing charge localization and chemical reactivity following photoionization in liquid water. *The Journal of Chemical Physics* **135,** 224510 (2011).
13. Svoboda, O., Hollas, D., Oncak, M. & Slavicek, P. Reaction selectivity in an ionized water dimer: nonadiabatic ab initio dynamics simulations. *Physical Chemistry Chemical Physics* **15,** 11531-11542 (2013).
14. Barran, P.E., Walker, N.R. & Stace, A.J. Competitive charge transfer reactions in small [Mg(H2O)N]2+ clusters. *The Journal of Chemical Physics* **112,** 6173-6177 (2000).
15. Band, A. *et al.* Characterization of Oxides of Cesium. *The Journal of Physical Chemistry B* **108,** 12360-12367 (2004).
16. Gomilšek, J.P., Kodre, A., Arčon, I. & Hribar, M. K-edge x-ray absorption spectra of Cs and Xe. *Physical Review A* **68,** 042505 (2003).
17. Weller, M.T., Henry, P.F. & Light, M.E. Rapid structure determination of the hydrogen-containing compound Cs2C2O4.H2O by joint single-crystal X-ray and powder neutron diffraction. *Acta Crystallographica Section B* **63,** 426-432 (2007).
18. Evans, J.C. The peroxide-ion fundamental frequency. *Journal of the Chemical Society D: Chemical Communications***,** 682-683 (1969).
19. Li, J. & Davis, R.J. Raman Spectroscopy and Dioxygen Adsorption on Cs-Loaded Zeolite Catalysts for Butene Isomerization. *The Journal of Physical Chemistry B* **109,** 7141-7148 (2005).
20. Nemade, K.R. & Waghuley, S.A. Synthesis of stable cesium superoxide nanoparticles for gas sensing application by solution-processed spray pyrolysis method. *Applied Nanoscience***,** 1-6 (2017).
21. Bates, J.B., Brooker, M.H. & Boyd, G.E. Raman spectra of O−2 and O−3 ions in alkali-metal superoxides and ozonides. *Chemical Physics Letters* **16,** 391-395 (1972).

22. Ito, K. & Bernstein, H.J. THE VIBRATIONAL SPECTRA OF THE FORMATE, ACETATE, AND OXALATE IONS. *Canadian Journal of Chemistry* **34,** 170-178 (1956).
23. Föppl, H. Die Kristallstrukturen der Alkaliperoxyde. *Zeitschrift für anorganische und allgemeine Chemie* **291,** 12-50 (1957).
24. Dudarev, V.Y.T., A.B.; Dobrolyubova, M.S. On phase transitions in rubidium and cesium epiperoxides. *Kristallografiya* **18,** 759-763 (1973).
25. Howell, R.W. Auger processes in the 21st century. *International Journal of Radiation Biology* **84,** 959-975 (2008).
26. Jahnke, T. *et al.* Experimental Observation of Interatomic Coulombic Decay in Neon Dimers. *Physical Review Letters* **93,** 163401 (2004).
27. Müller, C., Voitkiv, A.B., López-Urrutia, J.R.C. & Harman, Z. Strongly Enhanced Recombination via Two-Center Electronic Correlations. *Physical Review Letters* **104,** 233202 (2010).

Acknowledgments

We gratefully acknowledge support from the Department of Energy National Nuclear Security Administration (DOE-NNSA) under Award Number DE-NA0002912. We also acknowledge support from the DOE Cooperative Agreement No. DE-FC08-01NV14049 with the University of Nevada, Las Vegas. Portions of this work were performed at HPCAT (Sector 16), Advanced Photon Source (APS), Argonne National Laboratory. HPCAT operations are supported by DOE-NNSA under Award No. DE-NA0001974 and DOE-BES under Award No. DE- FG02-99ER45775, with partial instrumentation funding by NSF. APS is supported by DOE-BES, under Contract No. DE-AC02-06CH11357. Sandia National Laboratories is a multi-mission laboratory managed and operated by National Technology and Engineering Solutions of Sandia, LLC., a wholly owned subsidiary of Honeywell International, Inc., for the U.S. Department of Energy's National Nuclear Security Administration under Contract DE-NA0003525.

Authors Contributions

E.E., P.C., D.G. and M.P. carried out the experiments. E.E. and D.G. analyzed the data. E.E., E.K., M.P. contributed to data interpretation. E. K. and P.W. conducted the first-principle calculations. E.E. conceived the idea of electronic cascades in multitype bounded matter. E.E., D.G. and M.P. wrote the manuscript.

Author Information

The authors declare no competing financial interests. Correspondence and request for materials should be addressed to E.E. (egor.evlyukhin@unlv.edu) and M.P. (pravica@physics.unlv.edu).